Time Variant Interval Linear Programming for Environmental Management Systems

Z. Xiao[1, 2], J. Y. Du[1 *], Y. Guo[2], X. Li[2], and L. Guo[3]

[1] School of Computer and Information Engineering, Central South University of Forestry and Technology, Changsha 410004, China
[2] College of Information Science and Engineering, Hunan University, Changsha 410082, China
[3] National Nuclear Emergency Response Technical Assistance Center, Beijing 100037, China

ABSTRACT. Optimization technology is widely applied to maximize economic profit under ecology constrains in environmental management systems. To tackle the inherent uncertainties, inexact optimization methods have been proposed. Interval linear programming (ILP) model has drawn increasing scholarly attention. ILP model describe uncertainty by one coarse scaled stochastic process. However, uncertainty often involves multiple stochastic processes when zooming into high resolution. ILP model may not satisfied fine scale constraints. A time variant interval linear programming (TVILP) model is developed to implement temporal downscaling, and likewise, a heuristic algorithm integrating dynamic programming is proposed for Markov chained TVILP. Dynamic programming can converts time complexity exponential to polynomial. In the current paper, the performance of TVILP model is analyzed based on the following three metrics: maximal profit (M_profit), constraint violation risk (CVR), and maximal profit path risk (MPR). The performance of TVILP is further compared with the performance of Best and Worst method, the classic ILP model, Interval linear programming contractor, and Interval-parameter multi-stage stochastic linear programming. Experimental results reveal that TVILP provides refined solutions on a smaller granularity whose decision space contracts based on the most possible transition paths. Unable to obtain the maximum profit, though, TVILP does pose decreased constraint violation risk and maximal profit path risk, facilitating more feasible and reliable decision-making on environmental management.

Keywords: decision making, environment management, inexact optimization, linear programming, robustness

1. Introduction

In pursuing sustainable development, people have always been confronted with dilemmas between economic profit and social or environmental cost (Fu et al., 2021; Zhai et al., 2021). Environmental management systems (EMS) regulate an organization in a comprehensive, systematic, planned, and documented manner, which has been frequently deployed to balance the two conflicting goals. Many applications, such as those for waste disposal and agriculture irrigation, are designed to minimize monetary cost under environmental constraints using programming methods (Ji et al., 2020; Li et al., 2021). Hence, optimization technologies play an important role in EMS.

Uncertainties are inherent in natural environment (Moeini and Soltani-nezhad, 2020; Li et al., 2020; Wang et al., 2021). To be specific, the amount of waste in a city is related to its socio-economic development; likewise, precipitation is related to climate change and human production activities in the region (Shrestha and Wang, 2020; Xu et al., 2021). These uncertainties may complicate the issue of optimization. It is unlikely to optimize the problem just by ignoring these uncertainties, as it

can lead to inaccurate or even wrong decisions. Therefore, adopting an accurate optimization method to study EMS is essential. In previous studies, linear programming (LP) method was employed to optimize production management of factories and manufacturers (Hung et al., 1996), which was later extended to environmental engineering (Daniel et al., 1997; Chang et al., 2001), becoming a dominant optimization technology in EMS. Unlike production management, there exist quite a few uncertainties in environment-oriented management, including rainfall in agriculture irrigation and waste volume in waste disposal. Therefore, inexact LP models and methods have been constantly researched and developed. For instance, robust optimization (Beyer and Sendhoff, 2007) has emerged, immune with respect to parameter drifts, model sensitivities and others.

The inexact programming methods rely on probability distribution or membership function; however, it is not easy to acquire relevant knowledge. Alternatively, adaptive strategy can be employed (Zhu et al., 2012); however, given the real-time sudations, the adaptive strategy is not appropriate in terms of budgeting. The upper and lower bounds are quite straight forward in describing a random variable. Huang et al. (1992) proposed grey linear programming approach for municipal solid waste management plan for municipal solid waste management and found the two-step method (TMS) is effective in solving interval linear programming (ILP) problems. However, TMS could cause constraint violations in its solution space, and ac-

*Corresponding author. Tel.: +(86)15874070214; fax: +(86)073188821907.
E-mail address: dujiayi@csuft.edu.cn (J. Y. Du).

cordingly, many improved methods have been proposed. Huang and Cao (2011) used a three-step method (ThSM) to implement the decision space based on the original space of the TSM solution restriction process. Wang and Huang (2014) proposed an improved solution method based on TSM (ITSM) to avoid solution violation by adding extra conditional constraints during the process of solving the sub-problems, which is better than TSM.

With the higher robustness in terms of reality orientation, ILP has been applied to many real-world EMS applications, such as waste management (Pires et al., 2011; Wu et al., 2015), water resources allocation (Lv et al., 2010; Nikoo et al., 2012), and energy systems management (Dong et al., 2012; Li et al., 2014). For instance, Guo et al. (2010) proposed an inexact fuzzy-chance-constrained two-stage mixed-integer linear programming (IFCTIP) approach integrating inaccurate planning, two-stage stochastic programming, integer programming and fuzzy stochastic programming into a general optimization framework before applying it into the flood management system. An ideal flood diversion scheme is obtained. Lv et al. (2011) proposed a two-stage inexact joint-probabilistic programming (TIJP) method based on two-stage stochastic programming and interval mathematical programming, which was effectively applied to controlling air pollution problems. Among them, many models are mixture of ILP and fuzzy or stochastic programming.

However, the above-mentioned inexact programming models are based on a coarse time scale. Either probability distribution or interval is estimated on the entire time span of the planning period. Uncertainty is time variant in most cases. Take rainfall for example; it is a different stochastic event under wet or dry seasons within a year. Based on a coarse scale, under-estimation or overestimation may occur for a finer scale. In this case, a coarse time scale can lead to an unrefined optimization policy. As shown in Figure 1(a), the solution space with a rougher range is obtained. Those models take a high risk at lower time resolution in terms of optimality and constraint violation, resulting in poor performance and even failure of EMS. Hence it is necessary to propose a small-scale model to obtain a more refined solution space, as shown in Figure 1(b). The solution space on each small scale is more accurate, which will be of help to decision making, and optimization.

Therefore, optimization under time variant uncertainty is investigated and the stochastic process is introduced into LP model, shaping into a time variant ILP model (TVILP). Its motivation results from the following features in real life: (1) the distribution is hard to be acquired due to physical or practical constraints, and (2) the distribution is not stable and instead changes as time goes by. It is assumed that our method lack such distribution information. The only input is the information about the intervals under stages and the transfer distribution between stages. The transfer distribution does not mean that the distribution of interval variables is known. For example, the distribution between seasons can be estimated; however, the specific seasonal or yearly precipitation distribution remains unknown.

For most EMS, uncertainty is likely to approach stationary when downscaled to a short period, though the specific distribution is still unknown. The segmented scales determine a temporally consecutive sequence of stationary sub-ILPs, which are linked to the objective function through transition probability matrix. Further, an algorithm based on TSM (Huang et al., 1992) and dynamic programming method is proposed to solve TVILP if the transition follows the law of Markov chain.

The rest of this paper is organized as follows. Section 2 reviews the ILP optimization model and some selected solutions. Section 3 explains the motivation for the current paper, while the formal definition of TVILP model is given in Section 4. Section 5 provides a fast-approximate algorithm for Markov-chained TVILP, followed by a summary of synthetic experiments described in Section 6. Section 7 concludes this paper.
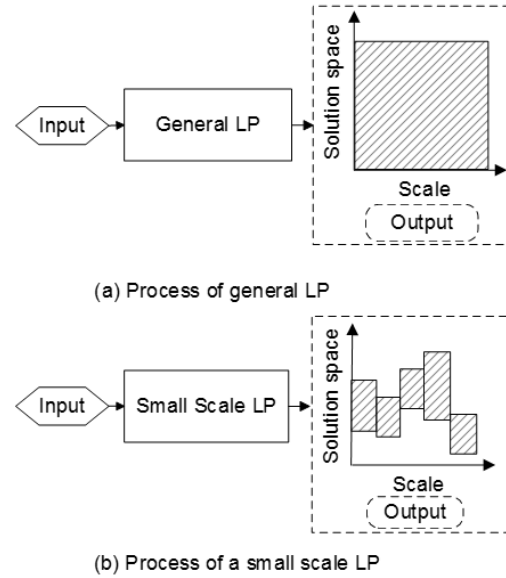

Figure 1. Process of different scale LP model: (a) Process of general LP, and (b) Process of a small scale LP.

2. Review of ILP

Uncertainty could be depicted by probability distribution, membership function, or interval. This paper focuses on interval uncertainty due to its loose hypothesis. In ILP, the coefficients are intervals whose upper and lower bounds are given, denoted by superscript "±". They could be any values within the intervals. Equation 1 shows the general form of ILP in EMS:

$$\text{Optimize:} \quad f\left(X\right) = C^{\pm} \cdot X^{\pm} \tag{1a}$$

subject to:

$$A^{\pm} X^{\pm} \leq b^{\pm} \tag{1b}$$

$$x_j^{\pm} \geq 0, \ \forall \ x_j^{\pm} \in X \tag{1c}$$

where $X^{\pm} = \{x_j^{\pm}\}^{n \times 1}$, $C^{\pm} = \{c_j^{\pm}\}^{1 \times n}$, $A^{\pm} = \{a_{ij}^{\pm}\}^{m \times n}$, $b^{\pm} = \{b_i^{\pm}\}^{m \times 1}$, n and m refer to the number of decision variables and constraints,

respectively.

For a deterministic combination of coefficients c_j, a_{ij} and b_i, Equation 1 becomes a traditional LP problem. An irregular polyhedron is obtained if all the possible combinations are taken into consideration, which is called ILP decision space (ILPDS). Some methods (Hladik, 2012a, 2012b) are developed to find ILPDS. The algorithm in (Hladik, 2012a) decomposed Equation 1 into 2^m sub-problems, which was improved by employing Beaumont formula (Hladik, 2012b) into a polynomial time algorithm.

Decision variables in the polyhedron ILPDS are interdependent, thus the solution is not straight for decision-makers of EMS, especially when there are quite a few decision variables. In engineering-oriented practice, many methods (Huang et al., 1992; Chinneck and Ramadan, 2000) decoupled the solution space from polyhedron to a hypercube with dependency removed. Best and Worst Analysis (BWS) (Chinneck and Ramadan, 2000) solves two extreme sub-ILPs, outputting the upper and lower bounds of each decision variables. A hypercube is expanded with decision variables sampled independently in their intervals.

It is demonstrated that part of the solutions in the decision space of BWS violate constraints, rendering high economic or social costs. Hence, a TSM (Huang et al., 1992) was proposed to mitigate constraint violation, which derived two improved sub-ILPs (Equations 2 and 3) from the initial ILP Equation 1:

Optimize: $\quad f^{\pm} = \sum_{j \in J_p} (c_j^{\pm} \cdot x_j^{\pm}) + \sum_{j \in J_n} (c_j^{\pm} \cdot x_j^{\pm})$ (2a)

subject to:

$$\sum_{j \in J_p} \left(sign\left(a_{ij}^{\pm}\right) \cdot \left|a_{ij}^{\pm}\right|^{-} \cdot x_j^{+} \right)$$
$$+ \sum_{j \in J_n} \left(sign\left(a_{ij}^{\pm}\right) \cdot \left|a_{ij}^{\pm}\right|^{+} \cdot x_j^{-} \right) \leq b_i^{+} \qquad (2b)$$

$i = 1, 2, \ldots, m$ (2c)

$x_j^{+} \geq 0, j \in J_p, x_j^{-} \geq 0, j \in J_n$ (2d)

where the superscripts $+$ and $-$ denote the upper and lower bounds of the interval, respectively. The function $sign(a_{ij}^{\pm})$ equals to 1 if $a_{ij}^{+} \geq a_{ij}^{-} \geq 0$ and -1 if $a_{ij}^{-} \leq a_{ij}^{+} \leq 0$. J_p and J_n are the subscript sets if $c_j^{+} \geq c_j^{-} \geq 0$ and $c_j^{-} \leq c_j^{+} \leq 0$, respectively.

Suppose that x_{jopt}^{+} and x_{jopt}^{-} are the solutions of ILP Equation 2, and then the other ILP Equation 3 will be obtained:

Optimize: $\quad f^{-} = \sum_{j \in J_p} \left(c_j^{-} \cdot x_j^{-} \right) + \sum_{j \in J_n} \left(c_j^{-} \cdot x_j^{+} \right)$ (3a)

subject to:

$$\sum_{j \in J_p} \left(sign\left(a_{ij}^{\pm}\right) \right) \cdot \left|a_{ij}^{\pm}\right|^{+} \cdot x_j^{+}$$
$$+ \sum_{j \in J_n} \left(sign\left(a_{ij}^{\pm}\right) \right) \cdot \left|a_{ij}^{\pm}\right|^{-} \cdot x_j^{-} \leq b_i^{-} \qquad (3b)$$

$i = 1, 2, \ldots, m$ (3c)

$x_{jopt}^{+} \geq x_j^{-} \geq 0, j \in J_p, x_j^{+} \geq x_{jopt}^{-}, j \in J_n$ (3d)

The two sub-ILPs above are traditional LPs, which can be solved by the simplex method. Sub-ILP Equation 2 corresponds to the optimistic one while Equation 3 is the conservative one. Many TSM-based methods, such as MILP (Modified Interval Linear Programming; Zhou et al., 2008), ThSM (Huang and Cao, 2011), RTS (Robust Two Step Method; Fan and Huang, 2012), and IRLP (Interval Recourse Linear Programming; Chen et al., 2015) were developed to further sidestep constraint violation.

3. Motivation

The interval parameters in the ILP model are estimated or predicted by the historic data. In this section, the precipitation from 2008 to 2014 at the city of Binzhou, Shandong province of China (Meng, 2016) is chosen and some statistical parameters are examined.

Figure 2 shows the precipitation distribution of different time scales. There exists a certain pattern for yearly distribution in the top of the figure. Therefore, a year-scale ILP can be solved. However, it may not be feasible in some cases. For example, if the government plants trees according to precipitation, and the growth period of the tree is one month which only depends on the rain, only the annual rainfall and determine the number of trees planted in the year can be estimated and determined. However, the number of trees planted per month remains unknown. Moreover, if the year 2009 is selected as an example, it can only be discerned that the precipitation varied seasonally. There was nearly no precipitation in the winter while the summer experienced many rainy days. Comparing May with July, one can find that there were more wet days in the former month, although with weaker intensity. Therefore, if the number of trees is distributed on a monthly basis, Figure 3 shows the ideal precipitation and the actual precipitation per month, which may result in the death of seedlings and economic losses. Therefore, a small-scale ILP problem is needed.

Tables 1 and 2 present the statistical results at two-time scales − year and month. In Table 1, "cor" represents the correlation coefficient of last year. Most of the correlation coefficients are over 0.9 except the 100-year-recurrence rainstorm in 2011, which validates the similar pattern over yearly distribution in Figure 2. The "sum" variable, representing the total precipitation each year, floats around 438.6 on average of seven years with standard deviation 44.5. Although the summed volume seems to fluctuate within 10%, "ave" and "stdev", which denote the average and standard deviation over twelve months, indicate an over 100% fluctuation as far as the monthly precipitation is concerned.

Table 2 illustrates the previous conclusion. "avg" and "stdev" in Table 2 denote the mean and standard deviation of the precipitation at monthly scale over seven years. The precipitation of a single month fluctuates with a smaller magnitude. However, the stochastic processes behave differently at monthly

Table 1. Statistics at Yearly Scale

Statistics	2008	2009	2010	2011	2012	2013	2014
sum	454.50	406.10	358.00	482.30	502.10	439.10	427.80
ave	37.86	33.84	29.83	40.19	41.84	36.59	35.65
stdev	50.40	45.70	37.80	68.20	63.80	48.90	45.50
cor	–	0.94	0.93	0.85	0.62	0.93	0.90
autocor-1st	0.71	0.73	0.65	0.41	0.50	0.62	0.69
autocor-2nd	0.15	0.15	0.17	-0.01	0.12	0.08	0.20

Table 2. Statistics at Monthly Scale

Statistics	Jan.	Feb.	Mar.	Apr.	May	Jun.	Jul.	Aug.	Oct.	Sep.	Nov.	Dec.
ave	0.00	0.00	0.04	3.04	43.70	113.78	140.68	84.50	10.33	41.70	0.77	0.00
stdev	0.00	0.00	0.10	1.96	17.85	49.70	42.55	25.18	5.66	15.92	1.25	0.00
cor	–	–	–	0.55	0.02	-0.06	-0.61	0.43	-0.20	-0.60	-0.64	–
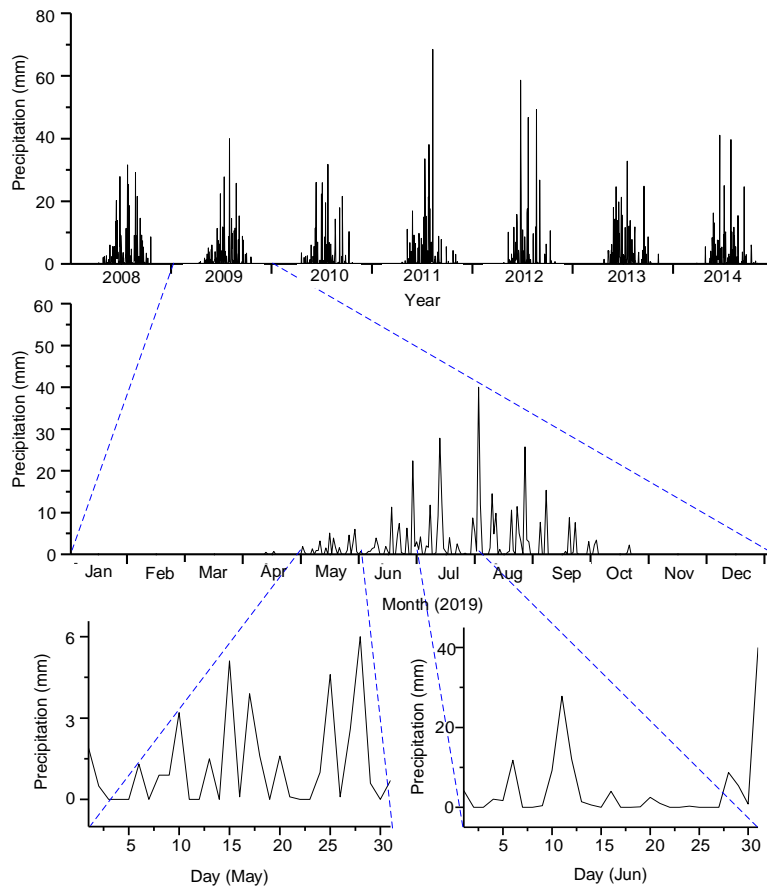
Figure 2. Precipitation distribution of different time scales.

scale and the correlation coefficients "cor" between two consecutive months are lower than 0.6, particularly for May, June and September. The precipitation distribution within one year exhibits different stochastic processes when downscaled monthly. Each stationary period corresponds to a different programming model. Meanwhile, the statistics of the precipitation on yearly scale may overestimate or underestimate the average monthly precipitation, resulting in constraint violation or regressive optimality. A refined optimization policy should be based on smaller granularity.

The last two rows of Table 1 show the first-order and second-order autocorrelation coefficients, respectively. Among all the seven years, the first-order autocorrelation coefficients are almost five times larger than the second-order ones. Therefore, the precipitation has first-order Markov property to some extent. That is, the precipitation depends much more on that of the previous two or more periods. The Markov chain can be used to model such stochastic process.

In addition to precipitation, many other environmental factors such as the length of sunshine and temperature, could lead to uncertainty. Meanwhile, the uncertainty often involves multiple stochastic processes. Therefore, when EMS problem involves these factors and a coarse-scale stochastic process jeopardizes the optimality and constrain satisfaction to describe uncertainty, it is necessary to propose a model of time variant ILP.
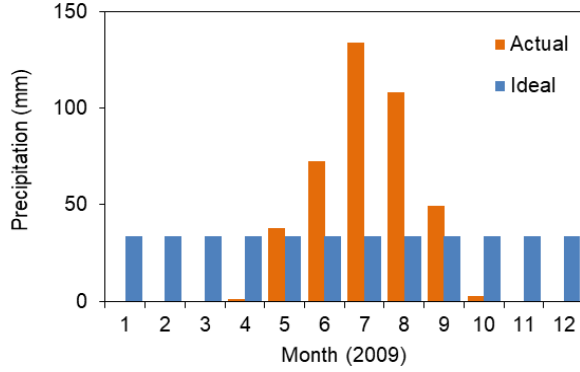

Figure 3. Ideal and actual precipitation in 2009.

4. Time Variant ILP Model

Because optimization problems involve multiple stochastic processes in its lifetime, policies should be time variant. Such refined decision helps decrease risks and improve practicality by tracking the dynamics in EMS.

Assume that T is the time span of planning period and $X(T)$ is the vector of decision variables for the optimization problem. If a stochastic variable is stationary during T, the optimization problem can be modeled as Equation 1. Considering time variance, assume that N is the number of stationary periods and the kth stationary period lasts for Δt_k, which satisfies $\sum_{k=1}^{N}\Delta t_k = T$. In order to achieve the optimization, a temporally consecutive sequence of stationary sub-ILPs is obtained after being downscaled to Δt_k.

In terms of the optimization process, $X(T)$ is divided into additive $X(s^{\Delta t_k})$ for a certain kind of stationary period during Δt_k, which is denoted by $s^{\Delta t_k}$, and $X(s^{\Delta t_k})$ is obtained by the model of a sub-ILP formulated as Equation 4:

Maximize: $f(s^{\Delta t_k}) = C^{\pm}(s^{\Delta t_k}) \cdot X^{\pm}(s^{\Delta t_k})$ (4a)

subject to:

$A^{\pm}(s^{\Delta t_k}) \cdot X^{\pm}(s^{\Delta t_k}) \leq b^{\pm}(s^{\Delta t_k})$ (4b)

$x_j \geq 0, \ \forall\, x_j \in X(s^{\Delta t_k})$ (4c)

When there is only one kind of stationary period during Δt_k, $X(T)$ is composed of $X(s^{\Delta t_k})$. However, there are multiple kinds of stationary periods in EMS in reality. Assume that $s^{\Delta t_k}$ denotes the set of all possible kinds of stationary periods during

Δt_k and $s_i^{\Delta t_k}$ denotes the ith one, where $\left|s^{\Delta t_k}\right|$ is the size of set $s^{\Delta t_k}$. The optimal path from Δt_1 to Δt_N has to be determined.

Equation 4 provides a solution space for $X(T)$ of smaller granularity. $X(T)$ is the combination of sub-solutions in the consecutive periods Δt_k. To support decision making, TVILP model needs to find a most-likely path. The TVILP model is given as Equation 5:

Maximize: $f = P\left(s_i^{\Delta t_1}, ..., s_i^{\Delta t_N}\right) \cdot \sum_{k=1}^{N}\left\{ C^{\pm}\left(s_i^{\Delta t_k}\right) X\left(s_i^{\Delta t_k}\right)\right\}$ (5a)

subject to:

$A^{\pm}\left(s_i^{\Delta t_1}\right) \cdot X\left(s_i^{\Delta t_1}\right) \leq b^{\pm}\left(s_i^{\Delta t_1}\right), \forall s_i^{\Delta t_1} \in S^{\Delta t_1}$

$\vdots$

$A^{\pm}\left(s_i^{\Delta t_N}\right) \cdot X\left(s_i^{\Delta t_N}\right) \leq b^{\pm}\left(s_i^{\Delta t_N}\right), \forall s_i^{\Delta t_N} \in S^{\Delta t_N}$ (5b)

$x(s_i^{\Delta t_k}) \geq 0, \ \forall x(s_i^{\Delta t_k}) \in X(s^{\Delta t_k})$, and $k = 1, 2, ..., N$ (5c)

$\forall s_i^{\Delta t_k} \in S^{\Delta t_k}$ and $i = 1, 2, ..., \left|S^{\Delta t_k}\right|$ (5d)

In fact, Equation 5 contains two optimizations. One is $X(s_i^{\Delta t_k})$, simply determined by sub-ILPs and defined as Equation 4, while the other is the path $<s_i^{\Delta t_1}, s_i^{\Delta t_2}, ..., s_i^{\Delta t_N}>$, which depends on the transition probability:

$P(s_i^{\Delta t_1}, ..., s_i^{\Delta t_N})$

$= P(s_i^{\Delta t_N} \mid s_i^{\Delta t_{N-1}}, ..., s_i^{\Delta t_1}) \cdot P(s_i^{\Delta t_1}, ..., s_i^{\Delta t_{N-1}})$

$= P(s_i^{\Delta t_1}) \cdot P(s_i^{\Delta t_2} \mid s_i^{\Delta t_1}) ... P(s_i^{\Delta t_N} \mid s_i^{\Delta t_{N-1}}, ..., s_i^{\Delta t_1})$

$= \prod_{k=1}^{N} P\left(s_i^{\Delta t_k} \mid s_i^{\Delta t_{k-1}}, ..., s_i^{\Delta t_1}\right)$ (6)

where $P(s_i^{\Delta t_k} \mid s_i^{\Delta t_{k-1}}, ..., s^{\Delta t_1})$ is the transition probability. The current period is related to all the previous stationary periods. If the transition probability matrix is known, $P<s_i^{\Delta t_1}, ..., s_i^{\Delta t_k}>$ will become computable.

It is assumed in this model that there is no cross impact between decision variables of individual sub-ILPs. Otherwise, the constraints of the sub-ILPs involve the previous decision variables. Equation 5 guarantees that the feasible field of decision variables is constraint violation free for any stationary periods.

The transition probability matrix reveals the interaction between sub-ILPs. The optimums of two succeeding sub-ILPs may be linked by weak transition probability. Consequently, those sub-ILPs should be excluded from $X(T)$.

If $<s_*^{\Delta t_1}, s_*^{\Delta t_2}, ..., s_*^{\Delta t_N}>$ is the optimal path, then $X(T) = \sum_{k=1}^{N} X(s_*^{\Delta t_k})$ is obtained.

Compared with the ILP model of Equation 1, the number of decision variables increases by N times and that of constraints in Equation 5 increases by $\sum_{k=1}^{N}\left|(s_*^{\Delta t_k})\right|$. The model becomes much more complicated due to smaller time granularity. Therefore, a refined optimization policy can be generated.

5. Viterbi-Based Algorithm for Markov-Chained TVILP

5.1. Algorithm Description

TVILP is of high computational cost, as the transition probability matrix involves a large number of possible paths. The time complexity of solving TVILP is O ($|s^{\Delta t_1}| \times |s^{\Delta t_2}| \times \cdots \times |s^{\Delta t_N}|$).

Many real-world situations, such as regional climates and rainfall, indicate that the most recent samples have more impact on the transition (Mieruch et al., 2010; Yoo et al., 2016). This is also validated in Section 3. It is of Markov property if the stationary period only depends on the elapsed one, i.e., $P(s_i^{\Delta t_k} | s_i^{\Delta t_{k-1}}, ..., s_i^{\Delta t_1}) = P(s_i^{\Delta t_k} | s_i^{\Delta t_{k-1}})$. Therefore, the Markov chain is a stochastic process that satisfies two hypotheses. Specifically speaking, the probability distribution of the system state $t+1$ is only related to state t, and state transition at $t+1$ is inde- pendent of the value of t. Since the Markov chain has a good predictive effect on the state of the process and all possible transitions generate a Markov chain, Equation 6 becomes $P(s_i^{\Delta t_k} | s_i^{\Delta t_{k-1}}, ..., s_i^{\Delta t_1}) = \prod_{k=1}^{N} P(s_i^{\Delta t_k} | s_i^{\Delta t_{k-1}})$.

Besides, addition in Equation 5 could be equivalent to multiplication, i.e., $\sum_{k=1}^{N} \{C^{\pm}(s_i^{\Delta t_i}) \cdot X(s_i^{\Delta t_i})\} \Leftrightarrow \prod_{k=1}^{N} \{C^{\pm}(s_i^{\Delta t_i}) \cdot X(s_i^{\Delta t_i})\}$. By substitution, the Markov-chained TVILP model could be formatted as Equation 7:

Maximize: $\quad f = \prod_{k=1}^{N} \left\{ P(s_i^{\Delta t_k} \mid s_i^{\Delta t_{k-1}}) \, C^{\pm}(s_i^{\Delta t_k}) \cdot X(s_i^{\Delta t_k}) \right\}$ (7a)

subject to:

$A^{\pm}\left(s_i^{\Delta t_1}\right) \cdot X\left(s_i^{\Delta t_1}\right) \leq b^{\pm}\left(s_i^{\Delta t_1}\right), \forall s_i^{\Delta t_1} \in S^{\Delta t_1}$
$\vdots$
$A^{\pm}\left(s_i^{\Delta t_N}\right) \cdot X\left(s_i^{\Delta t_N}\right) \leq b^{\pm}\left(s_i^{\Delta t_N}\right), \forall s_i^{\Delta t_N} \in S^{\Delta t_N}$ (7b)

$x(\Delta t_k) \geq 0, \forall x(\Delta t_k) \in X(\Delta t_k)$, and $k = 1, 2, ..., N$ (7c)

$\forall s_i^{\Delta t_k} \in S^{\Delta t_k}$ and $i = 1, 2, ..., |S^{\Delta t_k}|$ (7d)

Figure 4 demonstrates the transitions in Markov-chained TVILP. Two hypothetical stationary periods, s_o (before planning) and s_d (after planning) are added for describing the algorithm. Related transition probability is defined as $P(s_i^{\Delta t_1} | s_0) = P(s_i^{\Delta t_1})$, $\forall s_i^{\Delta t_1} \in S^{\Delta t_1}$ and $P(s_d | s_i^{\Delta t_N}) = 1$, $\forall s_i^{\Delta t_N} \in S^{\Delta t_N}$.

The symbol TVILP(s_o) is adopted to denote the problem of Equation 7. To solve TVILP(s_o), it is necessary to solve subproblems TVILP ($s_i^{\Delta t_1}$) prior to the boundary problems TVILP ($s_i^{\Delta t_N}$). The scale of stationary periods caused by TVILP(s_o) is N, while by TVILP ($s_i^{\Delta t_N}$) is 1.

TVILP involves two uncertainties which are the stochastic transition and interval fluctuation. The former will be addressed by maximum likelihood method while the latter will be solved by TSM described in Section 2. A dynamic programming algorithm based on the idea of the Viterbi algorithm is

developed to solve the Markov-chained TVILP, where backward computation is used to deal with sub-problems recursively and backtracking is further used to find the optimal path.
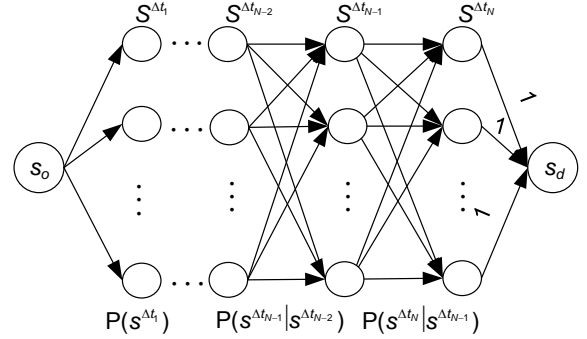

Figure 4. Transition in Markov-chained TVILP.

For stochastic transition in Markov-chained TVILP, the Viterbi algorithm is harnessed to find the maximum likelihood path with respect to a certain criterion. The criterion is defined by a function $G(C^{\pm}(s_i^{\Delta t_k}) \cdot X(s_i^{\Delta t_k}))$, which can be customized according to trade-off between constraint satisfaction risk and optimality. For instance, the conservative may prefer a path which ensures the maximal profit in the worst-case scenario by letting $G(C^{\pm}(s_i^{\Delta t_k}) \cdot X(s_i^{\Delta t_k})) = f^-$. f^- is obtained by solving Equation 3.

Two recursive functions Q and V are defined based on the alternative forms of objective function Equation 7. Q in Equation 8 represents the expected accumulative sum of G function for TVILP ($s_i^{\Delta t_k}$) based on TVILP ($s_i^{\Delta t_{k+1}}$). V of Equation 9 returns to the optimum, and the maximum likelihood stationary period $s_*^{\Delta t_k}$ is recorded in E in Equation 10:

$Q(s_i^{\Delta t_k}, X(\Delta t_k) \mid s_i^{\Delta t_{k+1}})$
$= G(C^{\pm}(s_i^{\Delta t_k}) \cdot X(\Delta t_k)) + P(s_i^{\Delta t_{k+1}} \mid s_i^{\Delta t_k}) \cdot V(s_i^{\Delta t_{k+1}})$ (8)

$V(s_i^{\Delta t_k}) = \max \left\{ Q(s_i^{\Delta t_k}, X(\Delta t_k)) \right\}$ (9)

$E(s_i^{\Delta t_k}) = \text{argmax}_{s_i^{\Delta t_{k+1}}} \left\{ P(s_i^{\Delta t_{k+1}} \mid s_i^{\Delta t_k}) \cdot V(s_i^{\Delta t_{k+1}}) \right\}$ (10)

In fact, Equations 9 and 10 define a series of new LP problems starting from Δt_N and generate a maximum likelihood path $< s_*^{\Delta t_1}, s_*^{\Delta t_2}, \cdots, s_*^{\Delta t_N} >$. At each stationary period $s_*^{\Delta t_i}$, a traditional ILP $< A^{\pm}(s_*^{\Delta t_i}), b^{\pm}(s_*^{\Delta t_i}), C^{\pm}(s_*^{\Delta t_i}) >$ is constructed as Equations 1 to 3 and further solved by TSM mentioned in Section 2. The complete algorithm in pseudo code is given in Algorithm 1.

Assume that there are M stationary periods during Δt_k at the maximum. Since the Viterbi algorithm is based on dynamic programming, the time complexity of this algorithm decreases to O($M^2 N$) and its space complexity increases to O(MN). It returns a temporal sequence of decision variables. Their values depend on the small-scale stationary periods of maximum likelihood. In contrast, the values of decision variables in tra-

ditional ILP are on a coarse scale, unaware of time variance. Consequently, the algorithm proposed in current paper can support more refined decision-making or reliable optimization.

Algorithm 1. Viterbi-based Algorithm for Markov Chained TVILP

Input:

$A^{\pm}(s_i^{\Delta t_k})$, $b^{\pm}(s_i^{\Delta t_k})$, $C^{\pm}(s_i^{\Delta t_k})$, $P(s_i^{\Delta t_k} \mid s_i^{\Delta t_{k+1}})$

Output:

$f^{\pm}$, $X^{\pm}(\Delta t_k)$

1: ARRAY **V**; ARRAY **E**; QUEUE **XQ**;
2: for $(k = N; k >= 0; k--)$ do
3:      for $(s_i^{\Delta t_k} \in S^{\Delta t_k})$ do
4:         Solve LP problem below:
             Maximize $r = G(C^{\pm}(s_i^{\Delta t_k}) \cdot X(\Delta t_k))$;
             s.t. $A^{\pm}(s_i^{\Delta t_k}) \cdot X(\Delta t_k) \le b^{\pm}(s_i^{\Delta t_k})$
5:          for $(s_j^{\Delta t_{k+1}} \in S^{\Delta t_{k+1}})$ do
6:              $Q = r + P(s_j^{\Delta t_{k+1}} \mid s_i^{\Delta t_k}) \cdot V(s_j^{\Delta t_{k+1}})$
7:              if $(Q > V(s_i^{\Delta t_k}))$ then
8:      $V(s_i^{\Delta t_k}) = Q$;
9:              $E(s_i^{\Delta t_k}) = s_j^{\Delta t_{k+1}}$;
10:             endif
11:         endfor
12:     endfor
13: endfor
14: $s_*^{\Delta t_1} = E(s^{\Delta t_0})$;
15: for $(k = 1; k >= N; k++)$ do
16: Solve ILP problem below by TSM:
           Optimize $f^{\pm}(\Delta t_k) = C^{\pm} s_*^{\Delta t_k} \cdot X^{\pm}(\Delta t_k)$
           s.t. $A^{\pm}(s_*^{\Delta t_k}) \cdot X^{\pm}(\Delta t_k) \le b^{\pm}(s_*^{\Delta t_k})$
17:     $f^{\pm} = f^{\pm} + f^{\pm}(\Delta t_k)$;
18:     XQ.enqueue $(X^{\pm}(\Delta t_k))$;
19:     $s_*^{\Delta t_{k+1}} = E(s_*^{\Delta t_k})$;
20: endfor
21: return $f^{\pm}$ and **XQ**;

5.2. Theoretical Analysis

TVILP model takes into account the transition probability between states. TVILP model uses a heuristic algorithm to obtain the maximum likelihood path. The profit sum of different paths is different, and so is the corresponding path possibility. There are three precipitation states during Δt_i, namely, high s_h, medium s_m, and rare s_r. There exists a probability distribution $\{Pr(s_h), Pr(s_m), Pr(s_r)\}$ over the possible states. The profit at state s_h will be obtained with probability $Pr(s_h)$; the profit at state s_m will be obtained with probability $Pr(s_h) + Pr(s_m)$, and the probability of the profit at s_r is $Pr(s_h) + Pr(s_m) + Pr(s_r)$. Hence,

the state cumulative distribution function (CDF) gives accumulated probability for precipitation $S \ge s$. Then CDF$(S \ge s_h) = Pr(s_h)$, CDF$(S \ge s_m) = Pr(s_m)$, and CDF$(S \ge s_r) = Pr(s_r)$ is offered.

Definition 1. Path Accumulated Profit (PAP): for a certain path p^{th} from start state to end state, we have PAP$(p^{\text{th}}) = \sum_{s \in p^{\text{th}}} \text{Profit}(s)$.

Definition 2. Path Confidence Level (PCL): for a certain path p^{th} from start state to end state, we have PCL$(p^{\text{th}}) = \min_{s \in p^{\text{th}}} \text{CDF}(S \ge s)$.

CDF$_i$ corresponds to the most likely state with PAP $- \Sigma_{ij=1}$ Profit $(s^{\Delta t_j})$ maximized for the pair (Profit$_i$, CDF$_i$) at $\Delta t_i (1 \le i \le N)$ stage, which is the maximum value in the current stage. For the current decision, the algorithm tries to choose the path according to max $\sum_{j=i+1}^{N} P(s^{\Delta t_j} \mid s^{\Delta t_{j-1}}) \text{Profit}(s^{\Delta t_j})$. Then for the pair (Profit$_{i+1}$, CDF$_{i+1}$) at $\Delta t_{i+1}(1 \le i \le N)$ stage, the CDF$_{i+1}$ still reaches the maximum value in the next state. Because the TVILP model is to select the most likely path, the PCL is still the highest.

6. Experiments

A synthetic scenario is used to validate the proposed algorithm. The government of Binzhou intends to improve the local environment, by planting two kinds of trees every year. Under the limited financial budget, the government must decide how many saplings to buy for the incoming year, so that the total profit can be maximized. For simplicity, it is assumed that the growth cycle of the two kinds of trees is one month and only depends on the precipitation. Once sufficient water is supplied, the trees can survive. Thus, the volume of precipitation is one constraint when making decisions. In addition, the yearly rate of green land should be kept at or above a certain level. The notations and values of relevant parameters are given in Table 3.

Most parameters in Table 3 are interval-values due to uncertainty. The precipitation is estimated based on the historical records described in Section 3. Because the rainfall uncertainty is time variant, 12 periods (Δt_1, Δt_2, ..., Δt_{12}) are divided as per calendar month for simplicity.

Referring to the analysis in Section 3, the precipitation can be categorized into rainless, rainy, pluvial, and flooding periods, which are denoted by s_l, s_m, s_h and s_r. Their corresponding interval values are [0.0, 10.0], [35.0, 52.0], [63.0, 98.0] and [116.0, 140.0], respectively. According to the seasonal feature of precipitation, Markov chain model of precipitation is obtained as shown in Figure 5. The parameter of green land rate GLR is also redefined at a smaller scale, given in Table 4.

6.1. Experimental Result

The optimization model at a coarse scale could be formulated as Equation 11:

Maximize: $C_A^{\pm} \cdot x_A^{\pm} + C_B^{\pm} \cdot x_B^{\pm}$ (11a)

subject to:

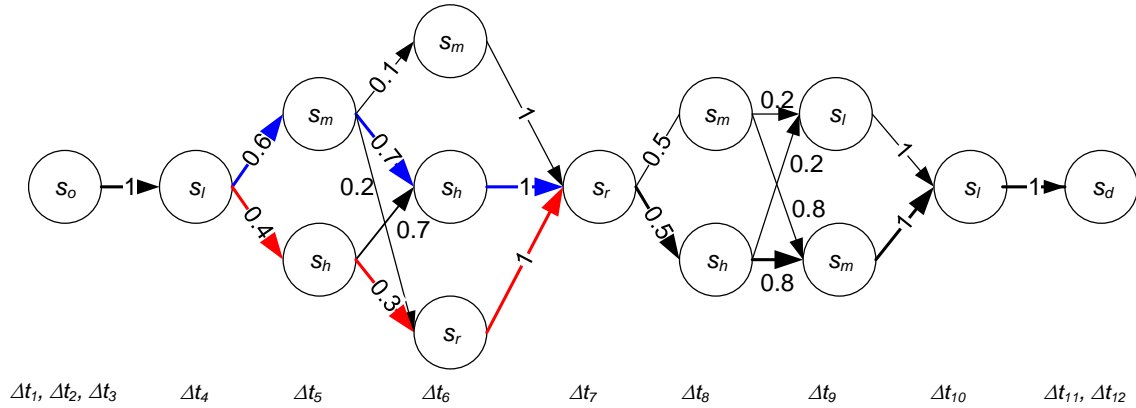Figure 5 (Markov chain model of precipitation):
States s_o, s_l, s_m, s_h, s_r, s_d with transition probabilities 1, 0.6, 0.4, 0.1, 0.7, 0.2, 0.7, 0.3, 0.2, 0.5, 0.5, 0.2, 0.2, 0.8, 0.8, 1, 1.

Time periods: $\Delta t_1, \Delta t_2, \Delta t_3$; Δt_4; Δt_5; Δt_6; Δt_7; Δt_8; Δt_9; Δt_{10}; $\Delta t_{11}, \Delta t_{12}$.

Figure 5. Markov chain model of precipitation.

Table 3. Notations and Values of ILP Parameters

Notation	Value	Unit	Description
$x_A^{\pm}$	decision variable		the number of saplings A
$x_B^{\pm}$	decision variable		the number of saplings B
$C_A^{\pm}$	[20.0, 35.0]	$	the net profit per plant A
$C_B^{\pm}$	[-13.0, -6.0]	$	the net profit per plant B
$W_A^{\pm}$	[3.8, 4.0]	m^3	the water demand of plant A
$W_B^{\pm}$	[0.5, 0.8]	m^3	the water demand of plant B
$Prec^{\pm}$	[394.0, 482.0]	mm	the precipitation per year
$Prec_i^{\pm}$	[0.0, 140.0]	mm	the precipitation of ith month
$GC_A^{\pm}$	[2.8, 4.2]	m^2	the green coverage of plant A
$GC_B^{\pm}$	[1.6, 2.5]	m^2	the green coverage of plant B
$GLR^{\pm}$	[60.0, 70.0]	%	the rate of green land
$AREA$	10,000.0	m^2	the area of planting field

Table 4. Green Land Rate at A Smaller Scale (%)

GLR	Δt_1	Δt_2	Δt_3	Δt_4	Δt_5	Δt_6	Δt_7	Δt_8	Δt_9	Δt_{10}	Δt_{11}	Δt_{12}
Period	Jan.	Feb.	Mar.	Apr.	May	Jun.	Jul.	Aug.	Sep.	Oct.	Nov.	Dec.
S_l	0	0	0	0	-	-	-	-	7	5	0	0
S_m	0	0	0	0	8	10	-	11	10	-	0	0
S_h	0	0	0	0	10	12	-	15	-	-	0	0
S_r	0	0	0	0	-	14	17	-	-	-	0	0

Tble 5. Decision Space based on Markov-chained TVILP

Periods	f^{+}				f^{-}			
	x_A^{-}	x_A^{+}	x_B^{-}	x_B^{+}	x_A^{-}	x_A^{+}	x_B^{-}	x_B^{+}
Δt_1	0	0	0	0	0	0	0	0
Δt_2	0	0	0	0	0	0	0	0
Δt_3	0	0	0	0	0	0	0	0
Δt_4	0	14	0	0	0	14	0	0
Δt_5	113	149	305	398	63	87	156	199
Δt_6	189	215	456	528	159	178	302	387
Δt_7	222	259	527	607	222	259	527	607
Δt_8	153	174	395	449	153	174	395	449
Δt_9	78	103	212	331	78	103	212	331
Δt_{10}	0	26	0	0	0	26	0	0
Δt_{11}	0	0	0	0	0	0	0	0
Δt_{12}	0	0	0	0	0	0	0	0

$$W_A^\pm \cdot x_A^\pm + W_B^\pm \cdot x_B^\pm \leq AREA \cdot Prec^\pm \qquad (11b)$$

$$GC_A^\pm \cdot x_A^\pm + GC_B^\pm \cdot x_B^\pm \leq AREA \cdot GLR \qquad (11c)$$

$$x_A^\pm \geq 0, x_B^\pm \geq 0 \qquad (11d)$$

Figure 6 presents the optimization result of model Equation 11 using TSM, which is described in Section 2. The black solid lines denote the two constraints of sub-ILP Equation 2, while the black dotted lines are constraints of sub-ILP Equation 3. (998, 1281) and (652, 2663) are the solutions of the two sub-ILPs, which further generate the decision space ($x_A \in [652, 998]$, $x_B \in [1281, 2663]$) as the red rectangle shows. The maximal profit under the optimistic case (998, 1281) is 27,244, while under the pessimistic case, it is -21579.
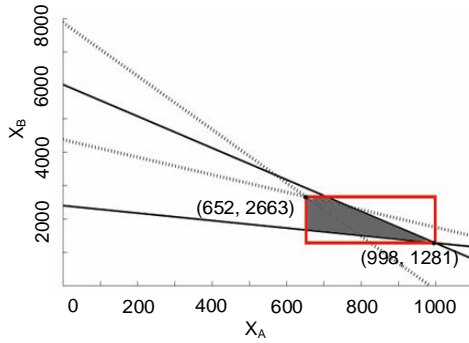
Figure 6. Optimization result at a coarse scale.

This problem is modeled as a Markov chained TVILP based on Table 4 and Figure 5, which is solved by the proposed algorithm. Two kinds of function G are tested, that is, f^- and f^+ of each small scaled ILP. In Figure 5, the lines in blue is the path when using f^-, whereas the red line is the path using f^+. Those two definitions represent pessimistic and optimistic attitudes towards decision-making. Take the transition between Δt_5 and Δt_6 for example, the optimistic one takes risk of a less possible transition due to the following high profit. The optimization model at a fine scale could be formulated as Equation 12:

Maximize:
$$\prod_{k=1}^{N} P(s_i^{\Delta t_k} \mid s_i^{\Delta t_{k-1}}) \Big(C_A^\pm(s_i^{\Delta t_k}) \cdot x_A^\pm(s_i^{\Delta t_k}) + C_B^\pm(s_i^{\Delta t_k}) \cdot x_B^\pm(s_i^{\Delta t_k}) \Big) \qquad (12a)$$

subject to:

$$W_A^\pm\left(s_i^{\Delta t_k}\right) \cdot x_A^\pm\left(s_i^{\Delta t_k}\right) + W_B^\pm\left(s_i^{\Delta t_k}\right) \cdot x_B^\pm\left(s_i^{\Delta t_k}\right)$$
$$\leq AREA \cdot Prec^\pm, \ k = 1, 2, ..., 12 \qquad (12b)$$

$$\sum_{K=1}^{12} \Big(GC_A^\pm\left(s_i^{\Delta t_k}\right) \cdot x_A^\pm\left(s_i^{\Delta t_k}\right) + GC_B^\pm\left(s_i^{\Delta t_k}\right) \cdot x_B^\pm\left(s_i^{\Delta t_k}\right) \Big)$$
$$\geq AREA \cdot GLR \qquad (12c)$$

$$x_A^\pm(s_i^{\Delta t_k}) \geq 0, x_B^\pm(s_i^{\Delta t_k}) \geq 0 \qquad (12d)$$

$$\forall s_i^{\Delta t_k} \in \{s_r, s_l, s_m, s_h\} \qquad (12e)$$
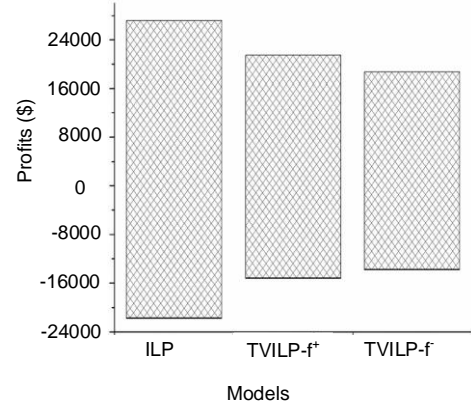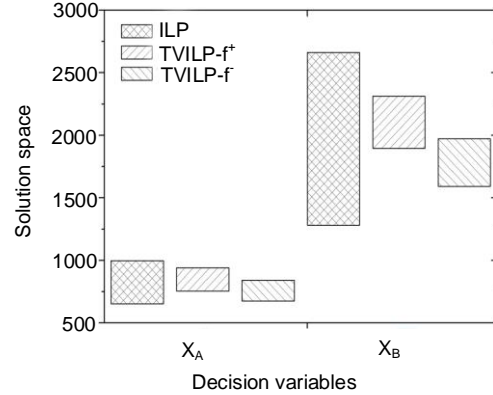

Figure 7. Optimality of three models.

Figure 8. Decision variables of three models.

The final decision spaces are displayed in Table 5. It comprises 12 time-divided sub-spaces, which are smaller in contrast with that in Figure 6. By downscaling, refined optimization policies are obtained. In order to verify the effectiveness of the proposed algorithm, the optimality of the solutions by three models is studied: ILP, TVILP-f^- and TVILP-f^+, which symbolize the classic ILP model at a coarse scale, time-variant ILP model with likelihood criteria f^- and f^+ respectively. Their decision spaces lead to intervals of profit.

Figure 7 presents the profit intervals, which indicates that ILP model has the largest interval compared with TVILP models. The maximal profit of ILP model entails a prediction that the monthly precipitation shall be maximal through the entire year. However, this probability is very small. The intervals of TVILP models are narrow, since only the most possible paths are considered. Besides, the likelihood criterion f^- is more conservative, leading to the smallest interval.

TVILP models output more reliable decisions, less likely to violate the constraints. Figure 8 presents the decision variables under the three models. The TVILP's spaces for each de-

cision variable are only part of the ILP's spaces. TVILP's spaces are prepared for what is most likely to happen under uncertain circumstances. By downscaling, decision risk can be properly reduced.

6.2. Result Analysis

Since the coefficients in the objective functions and the constraint functions are distributed over intervals, the decision variables are uncertain. This results in the risk of making uncertain decisions. Therefore, the performance of TVILP model is analyzed based on the following three metrics: Maximal profit (M_profit), Constraint violation risk (CVR), and Maximal profit path risk (MPR).

M_profit: It means the maximal profit in the generated decision space, which is formulated as Equation 13:

$$\text{M\_profit} = \text{Max}(f(X)) \ X \in DS \tag{13}$$

where $f(X)$ is the objective function, X is the decision variables, and DS is the decision space.

CVR: It means the risk that solutions in decision space violate constraints. The higher the value is, the more infeasible solutions are. This metric reflects the feasibility of the decision space, which is calculated according to the percentage of infeasible solutions, as shown in Equation 14:

$$CVR = size(IDS) \ / \ size(DS) \tag{14}$$

where DS is the decision space, IDS is the infeasible decision space, and $size(*)$ is the scope of any decision space.

MPR: Path risk is the risk caused by the decision making from coarse-scale to fine-scale. As shown in Figure 5, the probability of a path corresponds to the risk at which the profit is obtained. There may be many different paths for obtaining profits; however, there usually exists one unique path to get the maximal profit. In order to facilitate the calculation and comparison, this paper uses the maximal profit path risk. This metric can be formulated as Equation 15:

$$MPR = \prod_{k=1}^{N} \{ P(s_{\max}^{\Delta t_k} \mid s_{\max}^{\Delta t_{k-1}}) \} \tag{15}$$

where $s_{\max}^{\Delta t_k}$ is the state that the maximal profit path has passed during the kth stage, and $P(s_{\max}^{\Delta t_k} \mid s_{\max}^{\Delta t_{k-1}})$ is the transition probability from $s_{\max}^{\Delta t_{k-1}}$ to $s_{\max}^{\Delta t_k}$. This metric reflects the reliability of the decision space. If this value is smaller, the maximal profit can be obtained with greater probability; that is, the decision is more reliable.

From the perspective of these three metrics, the TVILP model is compared with other models and algorithms. The selected models and algorithms are: Best and Worst methods (BWS) (Chinneck and Ramadan, 2000), the classic ILP model (ILP) (Huang et al., 1992), Interval linear programming contractor (ILPC) (Hladik, 2012a), Interval-parameter multi-stage stochastic linear programming (IMSLP) (Li et al., 2006). These

four models are described in detail below:

1. BWS: This method gets the best optimum and the worst optimum, and the point settings of the interval coefficients that yield these two extremes. It provides the range of the optimized objective function, and the coefficients settings offer some insights into the likelihood of these extremes.

2. ILP: It has been described in detail in Section 2.

3. ILPC: It proposes an iterative method that finds an enclosure of the set of optimal solutions, and this method is based on a linear approximation and sequential refinement.

4. IMSLP: It corresponds to the lower and upper bounds of the desired objective in its solution process. It takes all possible state transitions or paths into account and provides intervals of decision variables for each state.

Among the aforementioned models, BWS, ILP and ILPC are coarse-scaled ones, while IMSLP and proposed model in the current paper are fine-scaled. However, as the IMSLP model assigns the decision variables to each state, its decision space is path-dependent. In contrast, our model only considers the most likely path.
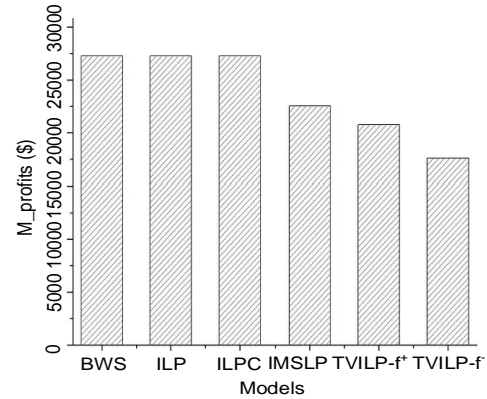

Figure 9. Maximal profit among different models.

6.2.1. Maximal Profit

Figure 9 presents the maximal profits of different models. The maximal profits of BWS, ILP and ILPC models are the highest. BWS and ILP contain larger decision space, and the case of ILPC is consistent with the optimal decision space. Take ILP for example; the point corresponding to the maximal profit locates at the bottom-left of the red rectangle in Figure 6. It lies in the decision space of BWS and ILPC; therefore, ILP, BWS and ILPC can be used to obtain the maximal profit. The decision space of all the possible paths can be calculated through the IMSLP model individually, including those paths of low possibility. Weighted averaging is performed based on the transition probability when calculating the range of decision variables. M_profit of IMSLP model is lower than that of the BWS model by 17% while the maximal profit value of TVILP model is lower than BWS model by 24 to 35%. This is because TVILP model only considers the most likely path, so that paths of higher profit but lower possibility are excluded. As for TVILP model, f^+ and f^- represent optimistic and pessimistic attitudes

towards decision-making. The optimistic one takes less risk of possible transition due to the following high profit. Therefore, the maximal profit of TVILP-f^+ is slightly higher than that of TVILP-f^-.
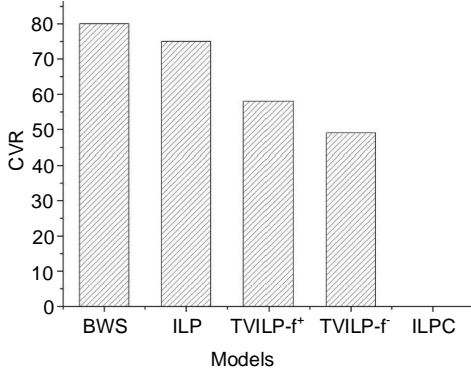

Figure 10. Percentage of infeasible solution of different models.

6.2.2. Constraint Violation Risk

Since there are only two decision variables in our experiment, the decision space is two-dimensional. In other words, the scope of the decision space can be represented by areas. As shown in Figure 7, the red rectangle represents the decision space, whose area is $Area_s = (x_A^+ - x_A^-)(x_B^+ - x_B^-)$. The shadowed field is the feasible decision space, whose area is $Area_f$ (calculated by integral). The risk can be calculated by Equation 16:

$$CVR = (area_s - area_f) / area_s \qquad (16)$$

The constraint violation risks of different models are given in Figure 10. As its decision space is path-dependent, IMSLP cannot be generalized on a coarse scale if the path is non-deterministic. Thus, this model is not chosen in this experiment. In addition, the decision space obtained by the ILPC model contracts to polyhedric ILPDS without infeasible solutions, therefore, it has no CVR.

BWS has the highest constraint violation risks. This model simply considers the best solution and the worst solution, which leads to a large area of decision space. Many solutions violate constraints. Although ILP improves BWS based on simple transformation, its decision space is still large and its CVR is slightly lower. Compared with BWS, the risk of constraint violation risk for TVILP is reduced by 18 to 26%. TVILP divides into small-scaled decision problems and models those sub-problems by ILP. The sub-ILPs exist non-zero CVR. Nonetheless, TVILP only takes into consideration the most possible state of each stage as a result, its decision space usually lies at the center of ILP's decision space as shown in Figure 8. Hence, its constraint violation risk is much lower.

6.2.3. Maximal Profit Path Risk

The maximal profit is closely related to the monthly precipitation, and the probability of the maximal profit path can be ob-

tained in accordance with precipitation transitions. As shown in Figure 5, the monthly precipitation is divided into four categories: s_l, s_m, s_h, and s_r, and the maximal profit corresponds to a path in the rainfall. BWS model was selected as the benchmark and normalized the MPR of different models. The normalization process is shown in Equation 17:

$$\text{Normalized MPR} = \frac{\text{MPR of BWS}}{\text{MPR}} \qquad (17)$$

Figure 11 shows the maximal profit path risk for different models after normalization. BWS, ILP, and ILPC have the same maximal profit path risk, because the maximal profit is obtained when the rainfall reaches its upper bound. Such probability is very low as it demands the largest monthly rainfall. For IMSLP, its path is selected by the user, although there is a unique path wherein each stage has the largest rainfall and gets the maximal final profit. However, the risk of this path is as high as that of BWS, ILP, and ILPC, because the likelihood for the monthly rainfall reaching the largest throughout the whole year is very slim. The MPR of TVILP is about a quarter of the benchmark model BWS. TVILP model only considers the most likely state in each stage, and thus the corresponding maximal profit will occur with a higher probability. Conse- quently, its risk is much lower. Further, there is one slight dif- ference between TVILP-f^+ and TVILP-f^-. Making decisions in an optimistic way, TVILP-f^+ tends to choose a path with smaller transition probability but more profit. In contrast, TVILP-f^- makes decisions in a pessimistic way.

6.2.4. Time Complexity

BWS and ILP solve the interval linear programming problem by converting it to two typical linear programming problems. Simplex algorithm is a common way of handing typical linear programming problems. The time complexity of simplex algorithm is $O(2^n)$ if there are *n* variables. Accordingly, the time complexity of BWS and ILP is $O(2^{n+1})$. ILPC runs in polynomial time. TVILP and IMSLP are both LP-based algorithms, of which the time complexity depends not only on the number of variables but also the number of states. The following experiment compares the complexity of TVILP and IMSLP.
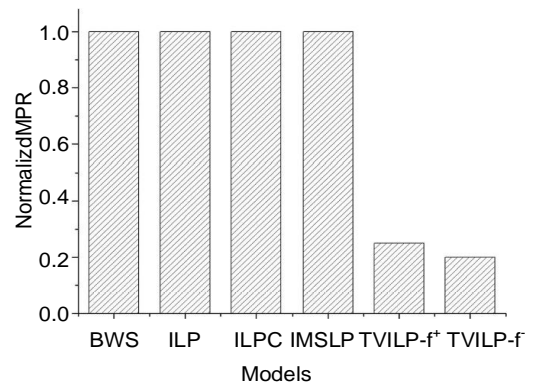

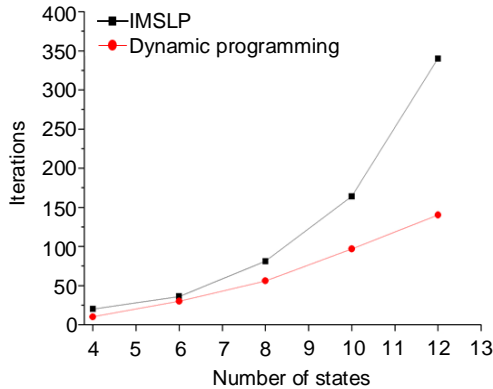**Figure 11.** Profit risk of different models.

Figure 12. Time consumption of IMSLP and ours.

For Markov-chained TVILP, a dynamic programming-based algorithm is proposed, which has much lower time complexity. This section will validate it under the same scenario. Previous experiments have analyzed the precipitation in terms of four stationary stochastic processes, and the transitions between the processes are shown in Figure 5. It includes 20 possible paths in all, while our algorithm only contains 10 iterations.

In order to further validate the time efficiency of our algorithm, more stochastic processes are divided. Figure 12 presents the time consumption of our algorithm and interval-parameter multi-stage stochastic linear programming under different number of states. The iterations of our algorithm increase polynomial, while the interval-parameter multi-stage stochastic linear programming has exponential tend.

Although our algorithm is time-efficient, too many states may make every path comparative and no overwhelming path exists. The decision space contracts to a small hyper-cube, which incurs more risk of constraint violations. This is the very issue we attempt to investigate in the future.

7. Conclusion

As for EMS, optimization technology has been commonly applied in balancing the conflict between economic development and ecological improvement. The optimization approaches under uncertainty such as ILP models ask for a stationary stochastic process, whilst a coarse scale of planning often involves multiple different stationary processes. In actual use, many decision variables in small-scale ILPs are dependent on time such as precipitation and temperature and the probability of stochastic process occurring may be similar to that of Markov model. Therefore, a TVILP model has been proposed based on Markov process, an algorithm is further adopted to obtain the optimal solution. Contributions of this paper can be summarized as follows:

1) Given the randomness of time variants, a Markov-chained TVILP model is developed, which provides a series of solutions at a smaller scale and supports more precise decision-making. Decision space contracts to a compact space which is oriented for the cases most likely to happen. In doing so, the constraint violation risks and path risk are decreased, thereby contributing to more feasible and reli-

able decisions.

2) A dynamic programming-based algorithm is proposed for Markov-chained TVILP, reducing the time complexity to polynomial one and improving its engineering friendliness.

3) The usefulness of the TVILP model is validated with a specific precipitation EMS example and verify the effectiveness of Viterbi-based algorithm for Markov-chained TVILP through a series of experiments.

It has to be admitted that there are two problems with TVILP. First, the original ILP is assumed to be dividable, and the decision variables are first calculated before considering other constraints. In some cases, however, sub-ILPs are interactive, under which TVILP and its algorithm should be amended. The other downside is the impact of the number of states on risk and optimality, and carrying out quantitative analysis of the impact is one direction for future studies.

References

Beyer, H.G. and Sendhoff, B. (2007). Robust optimization - a comprehensive survey. *Comput. Method Appl. M.,* 196(33-34), 3190-3218. https://doi.org/10.1016/j.cma.2007.03.003

Chang, G.W., Aganagic, M., Waight, J.G., Medina, J., Burton, T., Reeves, S. and Christoforidis, M. (2001). Experiences with mixed integer linear programming based approaches on short-term hydro scheduling. *IEEE T. Power Syst.,* 16(4), 743-749. https://doi.org/10.1109/59.962421

Cheng, G.H., Huang, G.H., Li, Y.P. and Dong, C. (2015). Interval recourse linear programming for resources and environmental systems management under uncertainty. *J. Environ. Inform.,* 30(2), 119-136. https://doi.org/10.3808/jei.201500312

Chinneck, J.W. and Ramadan, K. (2000). Linear programming with interval coefficients. *J. Oper. Res. Soc.,* 51(2), 209-220. https://doi.org/10.1057/palgrave.jors.2600891

Daniel, T. (1997). Linear programming models for the measurement of environmental performance of firms-concepts and empirical results. *J. Prod. Anal.,* 8(2), 183-197. https://doi.org/10.1023/A:1013296909029

Dong, C., Huang, G.H., Cai, Y.P. and Liu, Y. (2012). An inexact optimization modeling approach for supporting energy systems planning and air pollution mitigation in Beijing city. *Energy,* 37(1), 673-688. https://doi.org/10.1016/j.energy.2011.10.030

Fan, Y.R. and Huang, G.H. (2012). A robust two-step method for solving interval linear programming problems within an environmental management context. *J. Environ. Inform.,* 19(1), 1-9. https://doi.org/10.3808/jei.201200203

Fu, Y.P., Huang, G.H., Liu, L.R. and Zhai, M.Y. (2021). A factorial CGE model for analyzing the impacts of stepped carbon tax on Chinese economy and carbon emission, *Sci. Total Environ.,* 759, 143512, https://doi.org/10.1016/j.scitotenv.2020.143512

Guo, P., Huang, G.H. and Li, Y.P. (2010). An inexact fuzzy-chance-constrained two-stage mixed-integer linear programming approach for flood diversion planning under multiple uncertainties. *Adv. Water Resour.,* 33(1), 81-91. https://doi.org/10.1016/j.advwatres.2009.10.009

Hladik, M. (2012a). Interval Linear programming: A Survey, Nova Science Publishers, New York, chap *Linear Programming-New*

Frontiers in Theory and Applications, pp 85-120.

Hladik, M. (2012b). An interval linear programming contractor. *In: Proceedings of 30th International Conference Mathematical Methods in Economics*, Karvina, Czech Republic, pp 284-289.

Huang, G.H., Baetz, B.W. and Patry, G.G. (1992). A grey linear programming approach for municipal solid waste management planning under uncertainty. *Civ. Eng. Syst.,* 9(4), 319-335. https://doi.org/10.1080 /02630259208970657

Huang, G.H. and Cao, M.F. (2011). Analysis of solution methods for interval linear programming. *J. Environ. Inform.,* 17(2), 54-64. https://doi.org/10.3808/jei.201100187

Hung, Y. and Leachman, R.C. (1996). A production planning methodology for semiconductor manufacturing based on iterative simulation and linear programming calculations. *IEEE T. Semiconduct. M.,* 9(2), 257-269. https://doi.org/10.1109/66.492820

Ji, L., Huang, G.H., Niu, D.X., Cai, Y.P. and Yin, J.G. (2020). A stochastic optimization model for carbon-emission reduction investment and sustainable energy planning under cost-risk control. *J. Environ. Inform.,* 36(2), 107-118. https://doi.org/10.3808/jei.202000428

Li, G.C., Huang, G.H., Sun W. and Ding, X.W. (2014). An inexact optimization model for energy-environment systems management in the mixed fuzzy, dual-interval and stochastic environment. *Renew. Energ.,* 64(1), 153-163. https://doi.org/10.1016/j.renene.2013.11.013

Li, Y.P., Huang, G.H. and Nie, S.L. (2006). An inteval-parameter multi-stage stochastic programming model for water resources management under uncertainty. *Adv. Water Resour.,* 29(5), 776-789. https://doi.org/10.1016/j.advwatres.2005.07.008

Lv, Y., Huang, G.H., Li, Y.P., Liu, Z.F. and Cheng, G.H. (2010). Planning regional water resources system using an interval fuzzy bi-level programming method. *J. Environ. Inform.,* 16(2), 43-56. https://doi.org/10.3808/jei.201000177

Lv, Y., Huang, G.H. and Li, Y.P. (2011). A two-stage inexact joint-probabilistic programming method for air quality management under uncertainty. *J. Environ. Manag.,* 92(3), 813-826. https://doi.org/10.1016/j.jenvman.2010.10.027

Li, H.W., Li, Y.P., Huang, G.H. and Sun, J. (2021). Probabilistic assessment of crop yield loss to drought time-scales in Xinjiang, China, *Int. J. Climatol.,* https://doi.org/10.1002/joc.7059. In press.

Li, Z., Li, J.J. and Shi, X.P. (2020). A two-stage multisite and multivariate weather generator. *J. Environ. Inform.,* 35(2), 148-159. https://doi.org/10.3808/jei.201900424

Meng, X.Y. (2016). China meteorological assimilation driving datasets for the swat model version 1.0. *Cold and Arid Regions Science Data Center at Lanzhou*. http://www.cmads.org.

Mieruch, S., Noël, S., Bovensmann, H., Burrows J.P. and Freund J.A. (2010). Markov chain analysis of regional climates. *Nonlin Process. Geophys.,* 17(6), 651-661. https://doi.org/10.5194/npg-17-651-2010

Moeini, R. and Soltani-nezhad, M. (2020). Extension of the constrained gravitational search algorithm for solving multi-reservoir operation optimization problem. *J. Environ. Inform.,* 36(2), 70-81. https://doi.org/10.3808/jei.202000434

Nikoo, M.R., Kerachian, R. and Poorsepahy-Samian, H. (2012). An interval parameter model for cooperative inter-basin water resources allocation considering the water quality issues. *Water Resour. Manag.,* 26(11), 3329-3343. https://doi.org/10.1007/s11269-012-0074-5

Pires, A., Chang, N.B. and Martinho, G. (2011). Anahp-based fuzzy interval {TOPSIS} assessment for sustainable expansion of the solid waste management system in setbal peninsula, Portugal. *Resour. Conserv. Recy.,* 56(1), 7-21. https://doi.org/10.1016/j.resconrec.2011.08.004

Shrestha, N.K. and Wang, J. (2020). Water quality management of a cold climate region watershed in changing climate. *J. Environ. Inform.,* 35(1), 56-80. https://doi.org/10.3808/jei.201900407

Wang, F., Huang, G.H., Cheng, G.H. and Li, Y.P. (2021). Multi-level factorial analysis for ensemble data-driven hydrological prediction, *Adv. Water Resour.,* 103948, https://doi.org/10.1016/j.advwatres.2021.103948. In press

Wang, X.Q. and Huang, G.H. (2014). Violation analysis on two-step method for interval linear programming. *Inform. Sciences,* 281, 85-96. https://doi.org/10.1016/j.ins.2014.05.019

Wu, C.B, Huang, G.H., Li, W., Xie Y.L. and Xu, Y. (2015). Multi-stage stochastic inexact chance-constraint programming for an integrated biomass-municipal solid waste power supply management under uncertainty. *Renew. Sust. Energ. Rev.,* 41(1), 1244-1254. https://doi.org/10.1016/j.rser.2014.09.019

Xu, Z.P., Li, Y.P., Huang, G.H., Wang, S.G. and Liu, Y.R. (2021). A multi-scenario ensemble streamflow forecast method for Amu Darya River Basin under considering climate and land-use changes, *J. Hydrol.,* 598, 126276. https://doi.org/10.1016/j.jhydrol.2021.126276

Yoo, C., Lee, J. and Ro, Y. (2016). Markov chain decomposition of monthly rainfall into daily rainfall: Evaluation of climate change impact. *Adv. Meteorol.,* 2016, 1-10. https://doi.org/10.1155/2016/7957490

Zhai, M.Y., Huang, G.H., Liu, L.R., Guo, Z.Q. and Su, S. (2021). Segmented carbon tax may significantely affect the reginonal and national economy and environment- a CGE-based analysis for Guangdong Province. *Energy*, 231, 120958. https://doi.org/10.1016/j.energy.2021.120958

Zhou, F., Guo, H.C., Chen, G.X. and Huang, G.H. (2008). The interval linear programming: A revisit. *J. Environ. Inform.,* 11(1), 1-10. https://doi.org/10.3808/jei.200800105

Zhu, X.M., He, C., Li, K.L. and Qin, X. (2012). Adaptive energy-efficient scheduling for real-time tasks on dvs-enabled heterogeneous clusters. *J. Parallel Distr. Com.,* 72(6), 751-763. https://doi.org/10.1016/j.jpdc.2012.03.005